Eur Biophys J (1996) 24: 149–158

European Biophysics Journal

Normal coordinate analysis and vibrational spectra of 9-β-D-arabinofuranosyladenine hydrochloride (ara-A.HCl)

L. E. Bailey [1], A. Hernanz [1], R. Navarro [1], T. Theophanides [2]

[1] Departmento de Ciencias y Técnicas Fisicoquímicas, Universidad Nacional de Educación a Distancia, Senda del Rey s/n, E-28040 Madrid, Spain (Tel.: 34-1-3987377, Fax: 34-1-3986697, e-mail: ANTONIO.HERNANZ@HUMAN.UNED.ES)
[2] National Technical University of Athens, Chemical Engineering Department, Radiation, Chemistry and Biospectroscopy, Polytechnioupoli, Zografou, GR-15780 Athens, Greece

Received: 10 April 1995 / Accepted: 17 October 1995

Abstract. The vibrational spectra of a synthetic purine nucleoside with known antiviral activity, 9-β-D-arabinofuranosyladenine hydrochloride (ara-A.HCl) are reported. The Fourier transform infrared (FT-IR) and Fourier transform Raman (FT-Raman) spectra were recorded in the 4000-30 cm^{-1} spectral region. The harmonic frequencies and potential energy distributions (PED) of the vibrational modes of ara-A.HCl were calculated by two different methods: a classical molecular mechanics method and a semiempirical molecular orbital (MO) method, PM3. The results of both computational methods, based on the Wilson GF method, are compared with observed spectra, and an assignment of the vibrational modes of ara-A.HCl is proposed on the basis of the potential energy distributions (PED). It is found that the wavenumbers can be calculated with remarkable accuracy (≈1% deviation in most cases), with the classical mechanics method, by transferring a sufficiently large set of available harmonic force constants, thus permitting a reliable assignment. The semiempirical MO method, PM3, is found to be useful for the assignment of experimental frequencies although it is less accurate (≈10% deviation). IR intensities calculated by this method did not coincide with the experimental values. Certain out-of-plane vibrations in the base, not reported in previous studies, have been observed. The performance of both methods was related to the crystallographic and ab initio data available. Previous normal coordinate calculations for the adenine base and the nucleoside 5′-dGMP are compared with our results and discussed, in relation to the crystal structure of Ara-A.HCl.

Key words: Ara-A – Nucleoside – FTIR – FT-Raman – PM3

Introduction

Owing to the number of active compounds and their selectivity, nucleoside analogues and their derivatives are at present the most important group of antiviral drugs. While almost 25 years have elapsed since the first antiviral agent (5-iodo-2′-deoxyuridine) was marketed, the clinical use of antiviral agents has gained renewed interest and the search for new antiviral agents has been further boosted by the advent of AIDS (acquired immune deficiency syndrome) and the use of gene therapy GPAT (genetic prodrug activation therapy). It is clear that the need for treatment of viral diseases is enormous.

9-β-D-arabinofuranosyladenine (ara-A.HCl), Fig. 1, is a purine nucleoside that exhibits antiviral activity against DNA viruses of the herpes group. Suhadolnik (1970) has reviewed the biological activity of ara-A.HCl. The compound is curative against L 1210 leukaemia in mice when used in combination with inhibitors of adenosine deaminase, such as 2′-deoxycoformycin (Wilman 1990). Studies have indicated that the mechanism of action involves the conversion of ara-A by cellular kinases to the active

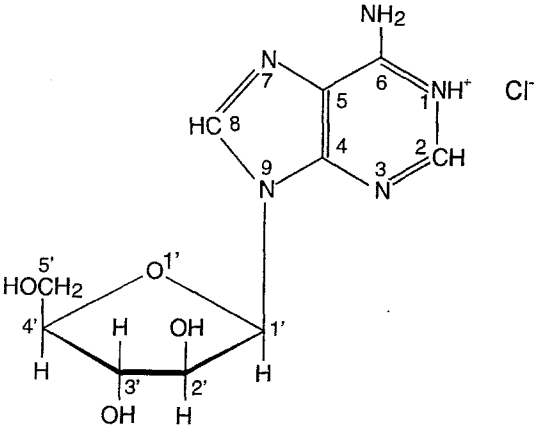

Fig. 1. Chemical structure and atomic numbering system of ara-A.HCl

Note: The cartesian coordinates corresponding to the PM3 optimized geometry can be obtained from the authors on request

Correspondence to: A. Hernanz

5′-triphosphate (de Clercq 1981) which has been shown to inhibit the viral DNA polymerase (Müeller et al. 1975). Ara-A can be incorporated into either cellular or viral DNA (Plunkett and Cohen 1975) although it may not necessarily affect the functioning of the DNA.

The crystal structure of ara-A.HCl has been studied by X-ray diffraction by Chwang and Sundaralingam (1974), who observed monoclinic crystals with unit cell dimensions of a=6.475 Å, b=15.787 Å, c=7.510 Å and β=121.62°, two molecules per unit cell, with $^3T_2$ puckering of the arabinose ring and [C(3′)-*endo-anti-gg*] conformation, which is one of the most common conformations found in ribo and 2′-deoxyribonucleosides. These authors observed intermolecular O(2′)...O(5′) hydrogen bonds linking adjacent molecules along the c axis; the sheets of adenine rings in adjacent unit cells linked by hydrogen bonds between the amino group and the ring nitrogen N(3); and the chloride ion located in the cavity formed by three nucleosides, to which it is hydrogen bonded through the arabinose O(3′), O(5′) and the amino nitrogen N(6). The structure of ara-A has been studied by Bunick and Voet (1974) and those of the natural analogue adenosine and adenosine.HCl by Lai and Marsh (1972) and Shikata et al. (1973), respectively.

Raman spectra of ara-A, ara-A.HCl, adenosine and adenosine.HCl have been reported by Theophanides et al. (1985) with assignments based on correlated group frequencies.

Because of the importance of adenine nucleosides in biochemistry, a greater understanding of their vibrational spectra is a useful basis in the study of both adenine-containing biopolymers and drug-enzyme interactions which would correlate antiviral and antitumour action with the physicochemical properties of nucleoside analogues.

Our purpose in this paper is to compare experimental FT-IR and FT-Raman frequencies with theoretical frequencies obtained by normal coordinate analysis using two different methods: a classical mechanics method and a semiempirical quantum mechanical molecular orbital (MO) method, PM3, and to evaluate the advantages of both methods for obtaining a reliable assignment of the vibrational spectra.

Assignments are thus proposed for observed frequencies corresponding to both in-plane and out-of-plane vibrations on the basis of PED. Previous normal coordinate analysis (Tsuboi et al. 1973; Majoube 1985a; Dhaouadi et al. 1993), partial ab initio molecular orbital calculations (Nishimura et al. 1982) and experimental spectra for the adenine base, and normal coordinate analysis of 5′-dGMP (Ghomi and Taillandier 1985) are compared with our results.

Experimental

Crystals of ara-A.HCl were obtained by slow evaporation of ara-A (Sigma) in equal volumes of toluene (Quimicen) and ethanol (Probus), adjusted to pH 2 with a trace of HCl (Probus).

The IR spectra of polycrystalline ara-A.HCl were recorded with a Bomem-DA3 spectrophotometer, working

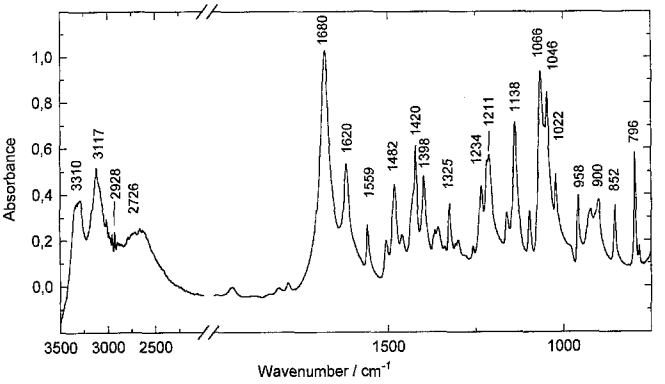

Fig. 2. FT-IR spectrum of polycrystalline ara-A.HCl in KBr disc (1.6 mg in 200 mg KBr) using Globar source and a narrow band MCT detector

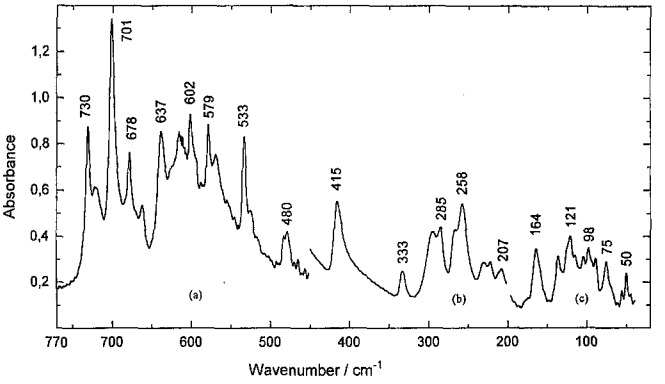

Fig. 3. Mid and far-IR spectra of polycrystalline ara-A.HCl. **a** 770-450 cm^{-1} region using Globar source, mid-IR DTGS detector and KBr disc (2 mg in 250 mg KBr). **b** 450-200 cm^{-1} region using Globar source, far-IR DTGS detector, 3 μm Mylar beam splitter and polyethylene disc (3 mg in 75 mg polyethylene). **c** 200-50 cm^{-1} region using high pressure mercury lamp, far-IR DTGS detector, 12 μm Mylar beam spliter and polyethylene disc (3 mg in 75 mg polyethylene)

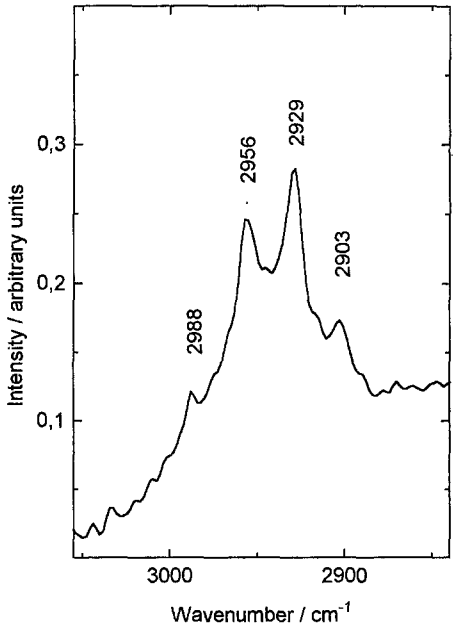

Fig. 4. FT-Raman spectra (3000 cm^{-1} region) of polycrystalline ara-A.HCl. The exciting wavelength was 1.06 μm and the apodized resolution was 4.0 cm^{-1}. An InGaAs detector at 77K was used

Table 1. Internal coordinates for the ara-A.HCl molecule (96 non-redundant and 27 redundant internal coordinates): ν=stretching, δ=in-plane bending, π=out-of-plane bending, τ=torsion

1 νN1-C2	32 νC5′-O5′	63 δN9-C1′-O1′	94 πC6-N6-H61-H62
2 νN1-H1	33 νC5′-H5′1	64 δC1′-O1′-C4′	95 πH2-C2-N1-N3
3 νN1-C6	34 νC5′-H5′2	65 δC1′-C2′-O2′	96 πN9-C1′-O1′-C2′
4 νC2-Hs	35 νO5′-HO5′	66 δC1′-C2′-C3′	97 τC2-N3-C4-C5
5 νC2-N3	36 δC6-N1-C2	67 δC1′-C2′-H2′	98 τC2-N1-C6-C5
6 νN3-C4	37 δC6-N1-H1	68 δO1′-C4′-C3′	99 τC6-N5-C4-N3
7 νC4-C5	38 δN1-C2-H2	69 δO1′-C1′-C2′	100 τC6-N1-C2-N3
8 νC4-N9	39 δN1-C2-N3	70 δC2′-O2′-HO2′	101 τC4-C5-C6-N1
9 νC5-C6	40 δN1-C6-C5	71 δC2′-C3′-C4′	102 τC5-N7-C8-N9
10 νC5-N7	41 δC2-N3-C4	72 δO2′-C2′-C3′	103 τC4-N9-C8-N7
11 νC6-N6	42 δC2-N1-H1	73 δO2′-C2′-H2′	104 τC5-C4-N9-C8
12 νN6-H61	43 δN3-C4-N9	74 δC2′-C3′-H3′	105 τC4-C5-N7-C8
13 νN6-H62	44 δN3-C2-H2	75 δC2′-C1′-H1′	106 τN1-C2-N3-C4
14 νN7-C8	45 δN3-C4-C5	76 δC2′-C3′-O3′	107 τC1′-O1′-C4′-C3′
15 νC8-H8	46 δC4-C5-C6	77 δC3′-O3′-HO3′	108 τC1′-C2′-C3′-C4′
16 νC8-N9	47 δC4-C5-C7	78 δO3′-C3′-C4′	109 τO2′-C2′-C1′-N9′
17 νN9-C1′	48 δC4-N9-C1′	79 δC4′-C3′-H3′	110 τHO2′-O2′-C2′-C1′
18 νC1′-H1′	49 δC5-C6-N6	80 δO1′-C4′-C5′	111 τHO3′-O3′-C3′-C4′
19 νC1′-O1′	50 δC5-C4-N9	81 δC3′-C4′-C5′	112 τHO5′-O5′-C5′-C4′
20 νC1′-C2′	51 δC6-C5-N7	82 δO1′-C4′-H4′	113 τC8′-N9′-C1′-C2′
21 νO1′-C4′	52 δC6-N6-H61	83 δC3′-C4′-H4′	114 τO1′-C1′-N9-C8
22 νC2′-O2′	53 δN1-C6-N6	84 δC4′-C5′-H5′2	115 τN1-C6-N6-H61
23 νC2′-C3′	54 δH61-N6-H62	85 δC4′-C5′-H5′1	116 νC1-H62
24 νC2′-H2′	55 δC5-N7-C8	86 δC4′-C5′-O5′	117 νC1-HO2′
25 νO2′-HO2′	56 δN7-C8-H8	87 δC5′-O5′-HO5′	118 νC1-HO5′
26 νC3′-O3′	57 δN7-C8-N9	88 δH5′1-C5′-H5′2	119 δH1′-C1′-O1′
27 νO3′-HO3′	58 δC8-N9-C4	89 δO5′-C5′-H5′2	120 τN1-C6-N6-H62
28 νC3′-C4′	59 δC8-N9-C1′	90 πC1′-N9-C8-C4	121 τO1′-C4′-C5′-O5′
29 νC3′-H3′	60 δN9-C1′-C2′	91 πH8-C8-N7-N9	122 τO1′-C4′-C5′-H5′1
30 νC4′-C5′	61 δN9-C1′-H1′	92 πN6-C6-N1-C5	123 τO3′-C3′-C4′-H4′
31 νC4′-H4′	62 δN9-C8-H8	93 πH1-N1-C2-C6	

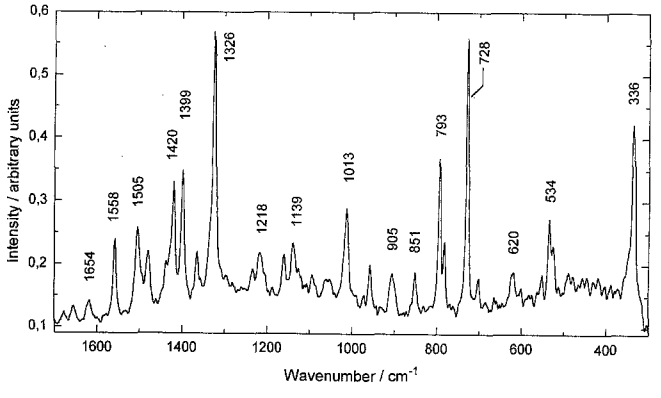

Fig. 5. Corrected FT-Raman spectra (1700-300 cm^{-1} region) of polycrystalline ara-A.HCl. Instrumental conditions as in Fig. 4

under vacuum (pressure ≤133.3 Pa) to eliminate IR absorption from water and CO_2. In the mid-IR region of 3500-750 cm^{-1}, Fig. 2, the spectrum was recorded with a Globar source, narrow band MCT detector and KBr beam splitter, using an effective apodized resolution of s = 1.77 cm^{-1} (RES = 2.0 and Hamming apodizing function), coadding 500 interferograms. The spectrum from 770 to 450 cm^{-1}, Fig. 3a, was recorded with a Globar source, DTGS detector and KBr beam splitter, using an effective apodized resolution of s = 0.89 cm^{-1} (RES = 1.0 and Hamming apodizing function), coadding 500 interferograms. In the region of 450-200 cm^{-1}, Fig. 3b, a Globar source and 3 μm Mylar beam splitter were used, whereas from 200 to 40 cm^{-1}, Fig. 3c, a high pressure mercury lamp and 12 μm Mylar beam splitter were used. These two spectra were recorded with a far-IR DTGS detector, resolution of s = 1.77 cm^{-1} (RES = 2.0 and Hamming apodizing function), coadding 1000 interferograms in order to obtain a satisfactory signal-to-noise ratio, S/N.

The FT-Raman spectra, Figs. 4 and 5, were obtained with a Bomem DA3 FT-Raman accessory. A krypton discharge lamp pumped Nd^{3+}:YAG laser (Quantronix CW114) working at 1.06 μm was the exciting source. The Raman emission was collected with 180° back-scattering geometry with an ellipsoidal mirror and passed through an adjustable iris with an aperture of 7 mm to the emission port of the interferometer. Two filters were used to prevent any stray light from the white light source and He-Ne laser contributing to the noise of the detector. Two plasma line filters allow only the 1.06 μm laser line to excite the sample. A quartz beam splitter and an indium gallium arsenide (InGaAs) detector operated at 77 K were installed. Raleigh line rejection was performed by a set of three notch filters at ≈17° with respect to the normal light beam. One of them was placed prior to the aperture at the emission port and the other two in the sample assembly close to the detector, before and after an iris with an aperture of 7 mm. The apodized resolution was s = 4.0 cm^{-1} (Blackman-Harris apodizing function). Correction for instrument response was made by division of the experimental spectra

with the spectrum of a white light lamp which had been normalized for source spectral radiance. The sample container was a glass tube with a spherical chamber of 7 mm diameter that had been back-silvered.

Computational methods

Classical mechanics calculations

The normal coordinate analysis is based on the Wilson GF method (Wilson et al. 1955). The cartesian coordinates were calculated from X-ray crystallographic data obtained by Chwang and Sundaralingam (1974). The G matrix was written in internal coordinate representation, using an extended basis of 123 internal coordinates. Table 1, including 27 redundancies which were eliminated by diagonalization, as their corresponding eigenvalues are zero.

The eigenvalues of G provided a "symmetry" coordinate basis which was then applied to the F matrix in internal coordinates to yield a "symmetrized" F matrix. The GF product results in the secular equation whose eigenvalues give the 96 harmonic vibration wavenumbers (3N-6 internal coordinates corresponding to the 34 atoms of the ara-A.HCl molecule).

The analysis was carried out using a computer program, Bioviban, developed by this research group (Escribano 1976; Orza et al. 1985). As a complete set of valence force constant values for ara-A.HCl was not found in the literature, the problem of selecting a suitable force field was overcome by transferring values published for smaller molecules. The valence force field, Tables 2 and 3, was transferred without modification from values published for adenine, assumed to be valid for the base residue (Dhaouadi et al. 1993), from guanine for the glycosidic bond and C-N-H bonds (Majoube 1984, 1985 b), 5′-dGMP (Ghomi and Taillandier 1985) and tetrahydrofuran (THF) (Eyster and Prohofsky 1974) for the arabinose moiety. It was assumed that the valence force field obtained for THF is also valid for the arabinose moiety of ara-A. It should be mentioned that THF has a planar ring of C_{2v} symmetry, while the arabinose ring of ara-A.HCl belongs to the C_1 point group. The conformation of the arabinose unit of ara-A.HCl is $^3T_2$ [C(3′)-endo, C(2′)-exo], one of the preferred puckering modes of the ribose ring.

Table 2. Diagonal valence force constants (in-plane and out-of-plane modes) for the set of 123 internal coordinates (including 27 redundancies) for ara-A.HCl: transferred directly from values published for adenine (Dhaouadi et al. 1993), guanine (Majoube 1984, 1985 b), 5′dGMP (Ghomi and Taillandier 1985) and tetrahydrofuran (Eyster and Prohofsky 1974). Units: stretching force constants (mdyn Å^{-1}); bending force constants (mdyn Å); out-of-plane wagging and torsional force constants (mdyn Å)

Stretch							
1	6.21	11	6.2	21	5.4953	31	4.6440
2	4.07	12	5.86	22	4.745	32	4.342
3	6.2	13	5.86	23	4.2697	33	4.644
4	5.13	14	7.00	24	4.5709	34	4.644
5	6.88	15	5.41	25	5.534	35	5.534
6	6.4	16	5.92	26	4.745	116	0.000
7	6.4	17	4.86	27	5.534	117	0.000
8	5.92	18	4.6440	28	4.2697	118	0.000
9	5.73	19	5.4953	29	4.5709		
10	5.51	20	4.2697	30	4.652		
Bend							
36	1.998	50	1.6	64	1.308	78	1.633
37	0.426	51	1.35	65	1.1633	79	0.656
38	0.520	52	0.415	66	1.0079	80	1.633
39	1.53	53	1.28	67	0.656	81	1.0079
40	1.29	54	0.452	68	1.1633	82	0.7810
41	1.9	55	1.68	69	1.1633	83	0.7346
42	0.426	56	0.425	70	0.530	84	0.7346
43	1.0	57	1.39	71	1.0079	85	0.7346
44	0.52	58	1.4	72	1.633	86	1.1633
45	1.231	59	0.31	73	0.781	87	0.533
46	1.0	60	1.588	74	0.656	88	0.550
47	1.23	61	0.52	75	0.7346	89	0.781
48	0.311	62	0.426	76	1.1633	119	0.7810
49	1.44	63	1.363	77	0.530		
Wag							
90	0.332	92	0.43	94	0.044	96	0.43
91	0.362	93	0.33	95	0.3		
Torsion							
97	0.257	103	0.55	109	0.010	115	0.0935
98	0.43	104	0.55	110	0.010	120	0.0208
99	0.585	105	0.55	111	0.010	121	0.0208
100	0.257	106	0.43	112	0.010	122	0.0208
101	0.455	107	0.010	113	0.100	123	0.0935
102	0.61	108	0.010	114	0.100		

Molecular orbital calculations

Semiempirical MO calculations were carried out using the PM3 Hamiltonians (Stewart 1989 a, b; 1991) as implemented in the HyperChem™ program (version 4, 1994). Geometry optimization for the G matrix was carried out by obtaining the minimum on the potential energy hypersurface, using the first derivative steepest descent method followed by the refined Polak-Ribiere conjugate gradient method. The AMBER molecular mechanics force field (Weiner et al. 1984, 1986), which takes hydrogen bonding into account, was used. The F matrix and subsequently the GF product, giving the vibrational frequencies, and their intensities were then calculated by the HyperChem™ program.

Results and discussion

Mid- and far-infrared spectra of polycrystalline ara-A.HCl in the 4000-750 and 770-40 cm^{-1} spectral regions are shown in Figs. 2 and 3. FT-Raman spectra are also shown in Fig. 4 and 5. Raman spectra of ara-A.HCl have been published previously (Theophanides et al. 1985), but frequencies in the 3000 cm^{-1} region were not measured. The internal coordinates are listed in Table 1. The fundamentals calculated with the Bioviban program and the semiempirical PM3 method, and assignment of the vibrational modes corresponding to ara-A.HCl together with the PED are listed in Table 4 and compared with the experimental

Table 3. Off-diagonal valence force constants (in-plane and out-of-plane modes) for the set of 123 internal coordinates (including redundancies) for ara-A.HCl: transferred directly from values published for adenine (Dhaouadi et al. 1993), guanine (Majoube 1984, 1985 b), 5′-dGMP (Ghomi and Taillandier 1985) and tetrahydrofuran (Eyster and Prohofsky 1974). Units: stretching force constants (mdyn $Å^{-1}$); bending, wagging and torsional force constants (mdyn Å); stretch-bend interaction force constants (mdyn)

Base (N1 protonated adenine) and glycosidic bond.							
Stretch-stretch (in-plane)							
9-8	0.1500	16-8	0.2000	14-10	0.9000	8- 7	0.1500
7-6	0.3500	11-9	0.7500	16-14	0.9000	14- 3	0.2200
7-9	0.4400	14-5	–0.1700	14- 8	–0.7100		
9-3	0.6500	14-7	0.1500	5- 1	0.5000		
3-1	0.6410	7-5	–0.1500	6- 5	0.2500		
10-9	–0.1500	5-3	0.1500	11- 3	0.8010		
Bend-bend (in-plane)							
49-40	–0.1000	53-40	0.3400	52-49	0.2000	53-52	0.2500
51-49	–0.4500						
Stretch-bend (in-plane)							
38-1	0.5400	46- 9	0.2000	50- 8	0.5500	58-17	–0.0300
45-7	0.7500	40- 9	0.2000	47- 9	–0.3000	44- 5	0.3500
46-7	0.7500	41- 5	0.7500	47-10	0.5500	51-10	0.7500
41-6	0.7010	39- 5	0.7500	53- 3	0.7800	55-10	0.7500
45-6	0.7010	40-11	0.9010	55-14	0.5800	48- 8	0.2700
36-1	0.7010	45- 7	0.3000	57-14	0.5800	62-16	0.7600
36-3	0.4000	50- 7	0.3000	57-16	0.5500		
39-1	0.7010	58- 8	0.5500	58-16	0.5500		
Wag-wag (out-of plane)							
94-92	–0.0300	95-91	0.0200	95-92	–0.0100		
Wag-torsion (out-of-plane)							
103-90	–0.0500	100-95	0.1150	101-92	0.1400	103-91	0.1200
104-90	0.2200	106-95	–0.0600	98-92	0.1100	102-91	–0.2450
Torsion-torison (out-of-plane)							
104-103	0.1950	101-99	–0.0800	103- 99	–0.0500	115- 98	–0.0100
104-102	–0.0500	106-98	0.0900	105-104	–0.1400	106- 97	–0.0400
99- 97	–0.1200	99-98	–0.0800	103-102	0.0350	106-100	0.0650
105-103	0.0500	106-99	–0.1000	105- 99	0.1000	100- 98	0.0200
102- 99	0.1200	101-97	0.1950	104- 99	0.2200	101- 98	0.0500
Arabinose ring and glycosidic bond							
Stretch-stretch							
21-19	0.2956	23-22	0.1010	28-23	0.1010	32-30	0.1010
20-19	0.1010	22-20	0.1010	30-28	0.1010	28-26	0.1010
28-21	0.1010	23-20	0.1010	26-23	0.1010		
Bend-bend							
69-63	–0.0410	69-67	0.0158	83-79	–0.0664	82-68	–0.0310
83-82	0.0363	74-66	–0.0520	75-67	0.0314	119-69	–0.0310
119-75	0.0363	74-71	–0.0520	82-64	0.0844	68-64	0.0285
73-67	0.0363	79-71	–0.0520	19-64	0.0844	69-64	0.0285
89-84	0.0363	83-71	–0.0310	79-68	0.0158	71-66	0.1139
79-74	0.0120	75-66	–0.0310	83-78	0.0158	81-71	0.1139
Stretch-bend							
82-21	0.3842	79-23	0.0703	78-26	0.4197	71-28	0.4170
89-32	0.3842	74-28	0.0703	86-32	0.4197	71-23	0.4170
73-22	0.3842	64-21	0.8752	68-28	0.3656	66-23	0.4170
75-20	0.4288	64-19	0.8752	69-20	0.3656	66-20	0.4170
83-28	0.4288	68-21	0.4197	65-20	0.3656	63-17	0.3470
74-23	0.3280	69-19	0.4197	72-23	0.3656	60-17	0.3470
79-28	0.3280	65-22	0.4197	76-23	0.3656		
67-20	0.3280	72-22	0.4197	78-28	0.3656		
67-23	0.0703	76-26	0.4197	86-30	0.3656		

Table 4. Observed and calculated wavenumbers for polycrystalline ara-A.HCl. Assignment (PM3) and potential energy distribution (PED, Bioviban) for the normal modes of vibration. Except for few modes, only PED values higher than 10% are mentioned. Intensities: s = strong, m = medium, w = weak, v = very, b = broad, sh = shoulder

Observed wavenumbers			Calculated wavenumbers		Potential energy distribution
IR $\tilde{\nu}$/cm^{-1}	FT-Raman $\tilde{\nu}$/cm^{-1}	Raman[a] $\tilde{\nu}$/cm^{-1}	PM3 $\tilde{\nu}$/cm^{-1}	Bioviban $\tilde{\nu}$/cm^{-1}	PED/%
3310bm			3431vw	3312	46νN6H62-45νN6H61 ($\nu_a NH_2$)
			3300vs		νO5′H + νO2′H (PM3)
			3228s		νO5′H − νO2′H (PM3)
			3518w	3204	47νN6H61 + 45νN6H62 ($\nu_s NH_2$)
				3159	97νC8H8
			3328s	3149	99νO3′H
3117bm				3149	60νO2′H + 40 νClHO2′
				3149	61νO5′H − 38νClHO5′
3009w			2960w	3077	96νC2H
2988w	2988w		3011vvw		ν_sC5′H$_2$ (PM3)
2972vw				2969	48νC5′H5′1 − 46νC5′H5′2 ($\nu_a CH_2$)
2952w	2956s		2942w		νO5′H (PM3)
2928w	2929s		2862vvw	2926	83νCl′Hl′
			2879vvw	2924	84νC4′H4′
	2903w		2900vvw	2902	59νC2′H2′ + 32νC3′H3′
2898w				2895	61νC3′H3′ − 35νC2′H2′
				2870	49νC5′H5′2 + 46νC5′H5′1 ($\nu_s CH_2$)
2726w			3385w	2725	97νNlH
			2746vs		νC8H and deformation of the base (PM3)
			2286s		νC3′H (PM3)
				1835	17δH61N6H62 + 16δC6N1H1 + 11δN1C6C5
				1781	71δH5′1C5′H5′2
1680vs	1677vvw		1771s	1686	17δN9C8H8 − 12δN7C8H8
			1667w		deformation of the vase (PM3)
	1654vvw		1647vw	1654	12δN3C4C5 − 9δN9C8H8
1620m	1617vw		1620w	1602	52δO5′C5′H5′2 − 34δC4′C5′H5′2
				1597	11δC5C4N9 + 11δC6N1H1
				1588	18τC6C5C4N3 − 12τC2N3C4C5
1559w	1558w	1560m	1535m	1544	39δC2N1H1 − 30δC6N1H1 + 15δH61H6H62
1505vw	1505w	1508m		1532	19δH1′C1′O1′ − 18δN9C1′H1′ + 12δH61N6H62
1482m	1480w	1483m		1489	30πH8C8N7N9
				1470	16πH8C8N7N9 − 15δN9C8H8 + 12δH1′C1′O1′
			1443vw	1455	22δN9C8H8 − 20δN7C8H8 + 12δH61N6H62
1420m	1420m	1422m		1419	28δH61N6H62scissoring − 8δC6N6H61
1398m	1399m	1401m	1401w	1401	34δC4′C5′H51′ + 6 δH61N6H62
				1387	33δH61N6H62scissoring − 13δC6N6H61
			1382vw	1381	24δC2′C1′H1′ − 22δN3C2H2 + 21δN1C2H2
1357vw	1364vw		1347vw	1344	13τO3′C3′C4′H4′
				1340	24τN3C2H2 − 17δN1C2H2
1325m	1326vs	1327s		1327	51δO2′C2′H2′ − 32δC1′C2′H2′
1300vvw				1307	18δN3C2H2 − 16δN1C2H2
				1279	14δN9C1′H1′ − 13δC2′C3′H3′
1234m	1233vvw		1254w	1239	20δO1′C4′H4′ + 16δC2′C3′H3′ − 12δC3′C4′H4′
				1229	20δC6N1H1 + 19δN7C8H8
1218m	1218vw	1219w	1218vw	1221	26δO1′C41H4′ − 17δC3′C4′H4′
1211m			1189vw	1204	22δC4′C4′H3′
			1175vw	1175	16δH1′C1′O1′ − 13δC2′C3′H3′
1161w	1160vw			1161	24δN7C8H8 − 18δN9C8H8 + 17δC4′C3′H3′
				1154	17δC3′C4′H4′ + 16δC4′C3′H3′
			1149vvw	1142	51πH1N1C2C6 − 10τC6N1C2N3
1138s	1139vw		1122vvw	1133	47πH1N1C2C6 − 9τC6N1C2N3
1096w	1094vvw		1109vw	1098	17δC2′C3′H3′
				1079	66δC5′O5′HO5′
1066s			1066vw	1070	19δC2′O2′HO2′ + 10δN7C8H8
1046s	1059bvvw		1049vw	1057	33δC5′O5′HO5′ + 18δC4′C5′H5′1
				1026	12δN7C8H8 − 11δC2N1H1
1022m	1013m	1015m	1024vw	1023	72δC3′O3′HO3′
			1000vw	987	29δC2′O2′HO2′ + 1δC3′O3′HO3′
958m	957vw			961	20δC5′O5′HO5′ + 19τO1′C4′C5′H5′1 + 10νC5′O5′
922w			919vw	919	11δN1C2N3

Table 4. Continued

Observed wavenumbers			Calculated wavenumbers		Potential energy distribution
IR $\tilde{\nu}$/cm^{-1}	FT-Raman $\tilde{\nu}$/cm^{-1}	Raman[a] $\tilde{\nu}$/cm^{-1}	PM3 $\tilde{\nu}$/cm^{-1}	Bioviban $\tilde{\nu}$/cm^{-1}	PED/%
900m	905vw		891vvw		
			878vw		
852m	851vw	850w	864vw	861	58δC2′O2′HO2′
				844	17πH2C2N1N3 – 11δC2′O2′HO2′
			834m	832	68πH2C2N1N3
796m	793m	796m		810	25τO3′C3′C4′H4′ – 13δC2′C3′H3′ + 13δC3′C4′H4′
783vw	782w		766vw	778	15τ03′C3′C4′H4′ – 11δC1′C2′H2′
730m	728vs	730s	757w	705	39πC6N6H61H62 – 37τN1C6N6H61
720w			715s	702	18πC6N6H61 – 13τN1C6N6H61 + 13πC6N6H61H62 – 10νC1H62
701vs	701vvw		697vw	697	24πC6N6H61H62 – 21τN1C6N6H61
678m				670	49πC6N6H61H62 – 19τN1C6N6H61 + 14τN1C6N6H62
662vw				650	45πC6N6H61H62 + 29τN1C6N6H62 – 6τN1C6N6H61
637m			638vw	640	24πC6N6H61H62 + 22τN1C6N6H62 + 12τO1′C4′C5′H5′1
616bm	620vvw	623w		626	53τO1′C4′C5′H5′1
602m			610vvw	609	12τN1C6N6H62 – 8τO1′C4′C5′H5′1
594sh			592vvw	587	33τO1′C4′C5′H5′1
579m			581vvw	580	32τN1C2N3C4 – 22τC6N1C2N3
569m	550vvw		553vvw	550	12πH8C8N7N9 – 11τO1′C4′C5′H5′1
533m	534w	537m		543	35νC1H62 – 32δC6N6H61 – 10δH61N6H62
	525vw		508vvw	514	23τO1′C4′C5′H5′1 + 21πH8C8N7N9
480w	489vvw		502vvw	487	12πH8C8N7N9 – 11δO2′C2′C3′
				468	22νC1H62 – 19πC6N6H61
			459vvw	465	11δC1′C2′C3′ + 10νC1H62
				433	46τN1C6N6H62 + 35τN1C6N6H61
415m				415	20πH8C8N7N9 – 18τC4C5N7C8 + 11τC5N7C8N9
			363vw	353	19τO3′C3′C4′H4′ – 15τO2′C2′C1′N9′ – 11δO3′C3′C4′
333vw	336s	337m	334m	335	31νC1H62 – 16τHO3′O3′C3′C4′ + 13τC1′O1′C4′C3′
				329	28τHO3′O3′C3′C4′ – 27νC1H62
294w				318	22τHO3′O3′C3′C4′ + 19νC1H62
285w			283vvw	289	51τHO3′O3′C3′C4′ + 16τO1′C4′C5′H5′1
266sh				278	17τC1′O1′C4′C3′ – 13νC1H62
258m					
230vw					
222vw					
207vvw			201vvw	198	68τHO5′O5′C5′C4′
			172vvw	194	16τHO2′O2′C2′C1′ + 15πN6C6N1C5
164w				151	93τHO3′O3′C3′C4′
				149	81τHO3′O3′C3′C4′
136w				136	89τHO5′O5′C5′C4′ – 10νC1HO5′
121m				118	79τHO2′O2′O2′C2′C1′ + 20νC1HO2′
115sh					
104vvw				101	14τO1′C4′C5′O5′ + 13τO1′C4′C5′H5′1
98vw					
89vw					
75vw				75	29τC8N9C1′C2′ + 29τO1′C1′N9C8 – 18νC1HO2′
55vvw			58vvw	57	25τO1′C4′C5′O5 + 19τO1′C4′C5′H5′1 – 14νC1HO2′
50vw				51	39τO1′C4′C5′O5′ + 31τO1′C4′C5′H5′1

[a] Theophanides et al. (1985)

results. Owing to the nature of the vibrational modes we present the calculated results for three distinct spectral regions:

3500-2000 cm^{-1} spectral region. In this region, bands due to O-H, N-H and C-H stretching vibrations are observed in the FT-IR and FT-Raman spectra of the polycrystalline sample. The two broad asymmetric bands observed in the FT-IR spectrum above 3000 cm^{-1} (Fig. 2) are due principally to overlap of N-H and O-H stretching modes. The observed broadening of these bands reveals the presence of hydrogen bonding as indicated by Chwang and Sundaralingam (1974) from X-ray diffraction data. Moreover, the wavenumber shift of the NH_2 stretchings from ≈3500 cm^{-1} for adenine in an argon matrix (Majoube et al. 1994) to ≈3300 cm^{-1} for polycrystalline ara-A.HCl provides additional evidence for the involvement of the NH_2 group in the hydrogen bonding. The calculated value of the asymmetric stretching vibration of this group, $\nu_a(NH_2)$, is observed at a higher wavenumber than the symmetric stretch-

ing, $\nu_s(NH_2)$, and agrees with published values for the adenine base (Dhaouadi 1993; Mohan 1993; Majoube 1985 a; Hirakawa 1985). Three different calculated fundamentals coincide at 3149 cm^{-1}, one of which is attributed to the O3′H stretching vibration and the other two to O2′H and O5′H stretching with contributions from stretching vibrations involving the Cl^- ion and adjacent H atoms. The aromatic and sugar C-H stretching modes are observed at lower wavenumbers, between 3000 and 2800 cm^{-1}, with lower intensities and half-band widths in the FT-IR spectrum. They are clearly seen in the FT-Raman spectrum, Fig. 4. The infrared peak at 3117 cm^{-1} does not coincide exactly with calculated fundamentals. It is not considered to be an overtone of the band at 1559 cm^{-1} because of the higher intensity of the former band. The broad band at 3117 cm^{-1} may therefore be assigned to calculated O-H stretching modes which would be expected to show similar profiles. The protonation of the basic site $N1H^+$ may be observed in the FT-IR spectrum by the stretching vibration of this positively charged group at 2726 cm^{-1}, which is strongly involved in intermolecular hydrogen bonding as observed in the X-ray crystal structure (Chwang and Sundaralingam, 1974).

1750-1000 cm^{-1} spectral region. Most of the observed FT-IR and FT-Raman peaks are due to in-plane vibration modes of the adenine moiety (Bertoluzza 1987; Dhaouadi 1993; Mohan 1993; Majoube 1985 a; Hirakawa 1985; Toyama 1994; Tsuboi 1987) although there are significant contributions from internal coordinates of the sugar ring in many of the normal modes. Consequently, the bands observed at ≈1672 cm^{-1} in FT-IR and at ≈1675 cm^{-1} in Raman for adenine, which these authors assign to the NH_2 scissoring, are observed as small contributions to the 1654 cm^{-1} mode (PED 5%, Bioviban) and 1667 cm^{-1} mode (PM3). The NH_2 scissoring contributes to a greater extent to the modes at 1419 and 1387 cm^{-1} (Bioviban) and 1401 cm^{-1} (PM3). Intense bands observed in adenine spectra by the above mentioned authors at ≈1604 cm^{-1} in FT-IR and ≈1612 cm^{-1} in Raman shift to 1650 and 1657 cm^{-1}, respectively in adenine hydrochloride (Bertoluzza 1987). These bands would correspond to the very weak FT-Raman band of ara-A.HCl at 1654 cm^{-1} and it is assigned to a combination of numerous in-plane internal coordinates of the base. The intense band at 1330 cm^{-1} in the FT-IR and 1331 cm^{-1} in the FT-Raman spectra of adenine which are observed at 1325 cm^{-1} and 1327 cm^{-1} in the ara-A.HCl spectra and the calculated spectra at 1327 cm^{-1} are also assigned to a combination of internal coordinates both of the base and the arabinose moiety. The methylene $C5'H_2$ scissoring of nucleic acids gives a Raman band at ≈1420 cm^{-1} (Thomas 1993). This internal coordinate of the ara-A.HCl contributes mainly to the fundamental at ≈1401 cm^{-1}. The strong FT-Raman band at 1326 cm^{-1} is mainly due to arabinose bendings. Various CN stretchings contribute to a similar band observed in the IR and Raman spectra of adenine and adenine hydrochloride. Mathlouthi and Koenig (1986), on the basis of their studies on the vibrational spectra of carbohydrates, and Tsuboi et al. (1994) on the basis of their study on the deoxyribose vibrations of thymidine, have discussed the difficulties in assigning all of the observed IR and Raman vibrations. These difficulties are due to the presence of highly coupled modes between 1500 and 1200 cm^{-1} and combination bands which may overlap with those due to fundamental modes, and interact with one another, leading to distortion of the shapes of observed bands. Many of the bands observed in this region are due to H-C-H, C-O-H and *endo-* and *exo-cyclic* H-C-O and C-C-H bending vibrations and are highly coupled modes. The calculated wavenumbers are in fairly good agreement with experimental values in this region.

1000-150 cm^{-1} region. Most of the vibrational modes in this region are due to torsions and bendings involving hydrogen atoms. The FT-IR bands at 1066, 1046, 1022, 958, 900 and 852 cm^{-1} (Fig. 2) and the FT-Raman bands at 1013 and 851 cm^{-1} (Fig. 5) are assigned to fundamental vibrations of the sugar in agreement with previous studies (Theophanides 1985) although the contributions of the C3′O3′H, C2′O2′H and C5′O5′H bendings are of greater importance, according to the present study, than the CO and CC stretching vibrations. The C2H, C8H and NH_2 hydrogen wagging modes coupled to torsion modes give rise to six strong to medium bands in the 730 to 640 cm^{-1} spectral region (Fig. 3). The strong band at 730 cm^{-1} is assigned to ring-breathing vibrations (Thomas 1993) combined with out-of-plane torsions. Tul'Chinsky et al. (1976) named the range 800-600 cm^{-1}, "the region of crystallinity" owing to the effect of packing of the molecule in the crystal lattice. Fundamental modes at ≈534 and ≈336 cm^{-1} with important contributions from stretching vibrations of the Cl^- ion with a H atom of the NH_2 group may provide information on the interaction between the Cl^- ion and the base. Contributions of νClH(O2′) and νClH(O5′) with νO2′H and νO5′H, respectively are also predicted in the fundamentals at 3149 cm^{-1}. In the region below 200 cm^{-1}, most of the bands are due to torsions of the arabinose residue and lattice vibrations.

In general, very good agreement was observed between experimental and calculated wavenumbers with the classical molecular mechanics method, Bioviban (≈1% deviation in most cases). By means of the use of a reliable force field, with a sufficiently large number of harmonic force constants, which accounts for both low- and high-wavenumber vibrations (Dhaouadi 1993; Florian 1993) the vibrational normal modes may be predicted with remarkable accuracy. The agreement obtained with the semiempirical method PM3 was within 10%. The potential energy distribution, PED, which gives information about the relative contributions of the force constants to the potential energy of a normal mode, is often limited only to the diagonal terms of the F matrix. In our calculations, the contributions of force constants for different in-plane and out-of-plane coupled vibrations were included (Dhaouadi 1993). These provide off-diagonal elements, which are useful in the case of large molecules, such as ara-A.HCl. The effects of nonbonded interactions are recognized as the most serious restriction to the transferability of valence force fields (Palmö and Pietilä 1988) and the use of the molecular mechanics method with the Bioviban program, where the nonbonded interactions are taken expli-

citly into account, and included as part of the overall potential energy function resulted in very good agreement with experimental results. The semiempirical method, PM3, is helpful in the assignment of bands although there is less agreement with the wavenumbers of experimental spectra (10%). This is due to the fact that this method uses an optimized geometry for the isolated molecule in a vacuum and not the crystal structure obtained by X-ray diffraction, and also depends on the adequacy of the parameters used.

Acknowledgements. The authors thank the Universidad Nacional de Educación a Distancia for a postgraduate research grant to one of the authors (L. E. B.).

References

Bertoluzza A, Fagnano C, Tosi R, Morelli MA, Long DA (1987) Molecular interactions between ellectrophiles and nucleic acids. II. J Raman Spectrosc 18:83–92

Bunick G, Voet D (1974) Crystal and molecular structure of 9-β-D-arabinofuranosyladenine. Acta Crystallogr B30:1651–1660

Chwang AK, Sundaralingam M (1974) Crystal and molecular structure of a purine arabinonucleoside, 9-β-D-arabinofuranosyladenine hydrochloride. Acta Crystallogr B30:2273–2277

Clercq E de (1981) Nucleoside analogues as antiviral agents. Acta Microbiol Acad Sci Hung 28:289–306

Dhaouadi Z, Ghomi M, Austin J, Girling R, Hester R, Mojzes P, Chinsky L, Turpin P, Coulombeau C, Jobic H, Tomkinson J (1993) Vibrational motions of bases of nucleic acids as revealed by neutron inelastic scattering and resonance Raman spectroscopy. 1. Adenine and its deuterated species. J Phys Chem 97:1074–1084

Escribano R (1976) PhD thesis. Univ. Complutense, Madrid

Eyster J, Prohofsky EW (1974) The normal vibrations of tetrahyrofuran and its deuterated derivatives. Spectrochim Acta A 30: 2041–2046

Florian J (1993) Comments on "Vibrational motions of bases of nucleic acids by neutron inelastic scattering and resonance Raman spectroscopy. 1. Adenine and its deuterated species". J Phys Chem 97:10889

Ghomi M, Taillandier E (1985) Normal coordinate analysis of 5'dGMP and its deuterated derivatives. Eur Biophys J 12: 153–162

Hirakawa AY, Okada H, Sasagawa S, Tsuboi M (1985) Infrared and Raman spectra of adenine and its ^{15}N and ^{13}C substitution products. Spectrochim Acta 41A 172:209–216

HyperChem™ (1994) Release 4 program, Hypercube, Inc., Ontario, Canada

Lai TF, Marsh RE (1972) Crystal and molecular structure of adenosine. Acta Crystallogr B28:1982–1989

Majoube M (1984) Vibrational spectra of guanine. A normal coordinate analysis. J Chim Phys 81:303–315

Majoube M (1985 a) Vibrational spectra of adenine and deuterium-substituted analogues. J Raman Spectrosc 16(2):98–109

Majoube M (1985 b) Guanine residue: A normal coordinate analysis of the vibrational spectra. Biopolymers 25:1075–1087

Majoube M, Millié Ph, Lagant P, Vergoten G (1994) Resonance Raman enhancement for adenine and guanine residues. J Raman Spectrosc 25:821–836

Mathlouthi M, Koenig JL (1986) Vibrational spectra of carbohydrates. Adv Carbo Chem Biochem 44:7–89

Mohan S, Ilangovan V (1993) Vibrational spectra and normal coordinate calculations of adenine. Indian J Pure Appl Phys 31: 750–754

Müeller W, Rodhe H, Beyer R, Maidhof A, Lachmann M, Taschner H, Zahn R (1975) Mode of action of 9-β-D-arabinofuranosyladenine on the synthesis of DNA, RNA and protein in vivo and in vitro. Cancer Res 35:2160–2168

Nishimura Y, Tsuboi S, Kato S, Morokuma K (1982) in: Proceedings of the 8th International Raman Conference. Lascombe J, Huong P (eds) Wiley Heyden, Chichester, p 703

Orza JM, Escribano R, Navarro R (1985) Out-of-plane vibrational assignments and potential functions of pyrrole and its deuterated derivatives. J Chem Soc Faraday Trans 2 81:653–662

Palmö K, Pietilä LO (1988) Valence force fields as a tool in vibrational spectroscopy and molecular mechanics. Croat Chem Acta 61:605–620

Plunkett W, Cohen SS (1975) Antiviral activity of 9-β-D-arabinofuranosyladenine. 1. Cell Culture Studies. Cancer Res 35:415

Shikata K, Ueki T, Mitsui T (1973) Crystal and molecular structure of adenosine HCl. Acta Crystallogr B29:31–38

Stewart JP (1989 a) Optimization of parameters for semiempirical methods. I Method. J Comput Chem 10:(2)209–220

Stewart JP (1989 b) Optimization of parameters for semiempirical methods. II. Applications. J Comput Chem 10:(2)221–264

Stewart JP (1991) Optimization of parameters for semiempirical methods. III. J Comput Chem 12:(3)320–341

Suhadolnik RJ (1970) Nucleoside antibiotics. Wiley, New York

Theophanides T, Hanessian S, Manfait M, Berjot M (1985) Raman spectra of the arabinonucleosides ara-A and ara-C compared with the spectra of adenosine and cytidine. J Raman Spectrosc 16(1):32–38

Thomas GJ Jr, Tsuboi M (1993) Raman spectroscopy of nucleic acids and their complexes. In: Bush CA (ed) Advances in Biophysical Chemistry. Vol. 3. Jai Press, Greenwich, Connecticut, pp 1–70

Toyama A, Hanada N, Abe Y, Takeuchi H, Harada I (1994) Assignment of adenine ring in-plane vibrations in adenosine on the basis of ^{15}N and ^{13}C isotopic frequency shifts and UV resonance Raman enhancement. J Raman Spectrosc 25:623–630

Tsuboi M, Takahashi S, Harada I (1973) Infrared and Raman spectra of nucleic acids. Vibration in the base-residue. In: Duchesne J (ed) Physicochemical properties of nucleic acids, Vol 2. Academic Press, New York, pp 91–145

Tsuboi M, Nishimura Y, Hirakawa AY, Peticolas WL (1987) In: Biological applications of Raman spectroscopy. Spiro TG (ed), vol 2. John Wiley, New York, pp 163–165

Tsuboi M, Ueda T, Ushizawa K, Sasatake Y, Ono A, Kainosho M, Ishido Y (1994) Assignment of the deoxyribose vibrations: isotopic thymidine. Bull Chem Soc Jpn 67:1483–1484

Tul'Chinsky VM, Zurabyan SE, Asankozhoev KA, Kogan GA, Khorlin AY (1976) Study of the Infrared spectra of oligosaccharides in the region 1000-40 cm^{-1}. Carbohydrate Res 51:1–8

Weiner SJ, Kollman P, Case D, Singh V, Ghio C, Alagona G, Profeta S (1984) A new force field for molecular mechanics simulation of nucleic acids and proteins: AMBER. J Am Chem Soc 106:765–784

Weiner SJ, Kollman P, Nguyen D, Case D (1986) An all atom force field for simulation of proteins and nucleic acids. J Comput Chem 7:230–252

Wilman DE (1990) The chemistry of antitumour agents. Blackie, Glasgow, London, p 304

Wilson EB, Decius JC, Cross PC (1955) Molecular vibrations. McGraw Hill, New York